Structural properties of the Southern San Andreas fault around Thousand Palms, California, from analysis of large-N seismic array data

Pieter-Ewald Share[1]; Frank L. Vernon[2]; Yuri Fialko[2]; Amir A. Allam[3]; Yehuda Ben-Zion[4,5]

[1]Oregon State University, [2]University of California San Diego, [3]University of Utah, [4]University of Southern California, [5]Southern California Earthquake Center

Abstract

We present preliminary results from a large-N seismic nodal array deployment spanning the Banning and Mission Creek strands (BF and MCF) of the Southern San Andreas fault (SSAF) near the Thousand Palms Oasis Preserve, California. A number of key characteristics of the SSAF remain poorly known, including the fault attitude at depth, the extent of fault-related damage, partitioning of slip between active fault strands, and along-strike variations in shallow creep. Analyses of seismic waveforms from local, regional and teleseismic earthquakes recorded across the array are used to better understand the subsurface fault structure and properties.

Data and Methodology

The SSAF large-N nodal array consists of 322 3C 5 Hz Fairfield nodal geophones and recorded continuously at 500 sps for about a 5-week period. The array geometry comprises a ~4-km long profile spanning both BF and MCF strands and dense 2D arrays on the BF and MCF surface traces, respectively.

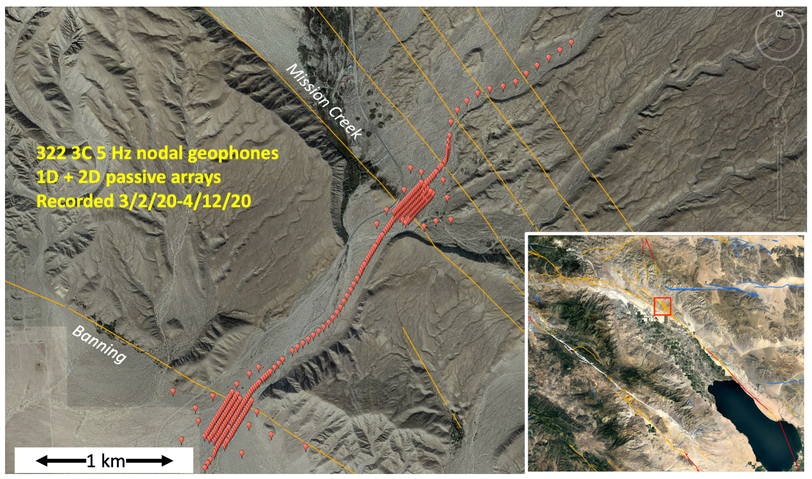

Figure 1: The SSAF Large-N nodal array spanning the merger of the BF and MCF strands around the Thousand Palms Oasis Preserve.

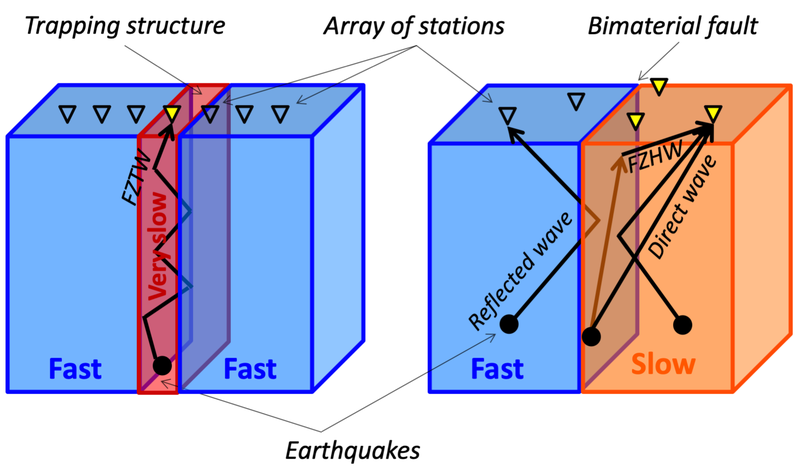

Using fault zone phases to infer fault structure

The presence of sharp seismic contrasts within and around a fault zone allows a plethora of direct, reflected, refracted and transmitted phases to be generated from incoming teleseismic, regional and local earthquake wavefields. We analyze the arrival, phase and amplitude characteristics of these phases, bearing in mind which earthquakes generate them and stations record them, to help constrain the geometric and structural properties of the local fault zone.

Teleseismic/Regional Earthquake Results

The longer wavelengths of regional and teleseismic earthquakes allow us to constrain large scale (~km) velocity variations across the array and fault zone, and, the locations of rapid changes in these large-scale structures. Several moderate to large regional and teleseismic earthquakes (right) occurred during the recording window. These wavefields are qualitative inspected for rapid changes in amplitude and phase (Figure 2) and their arrival time variations are quantified (Figure 3).

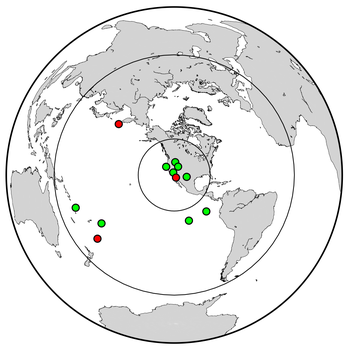

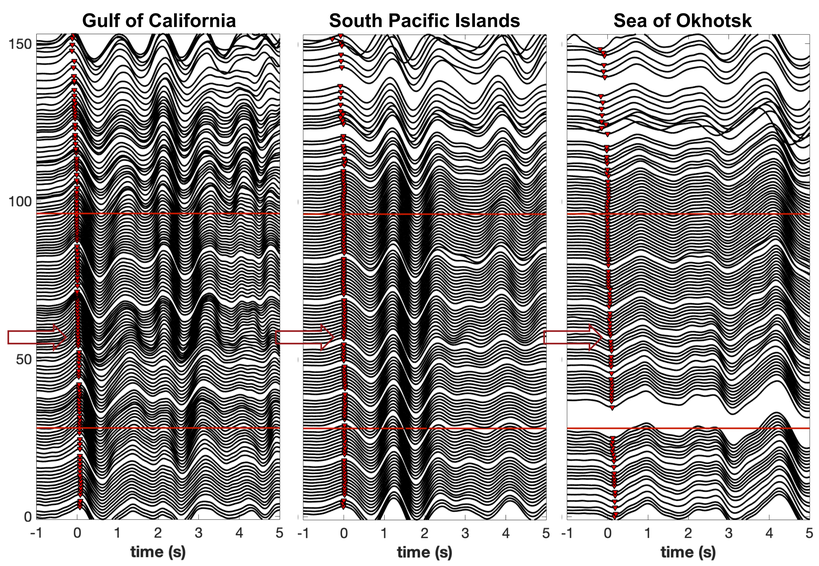

Figure 2: 1 HZ low-pass filtered P wavefields from representative regional and teleseismic earthquakes (red circles above). In addition to rapid changes in the wavefield around the BF and MCF there is another large-scale structural change around stations 50-60 (arrows).

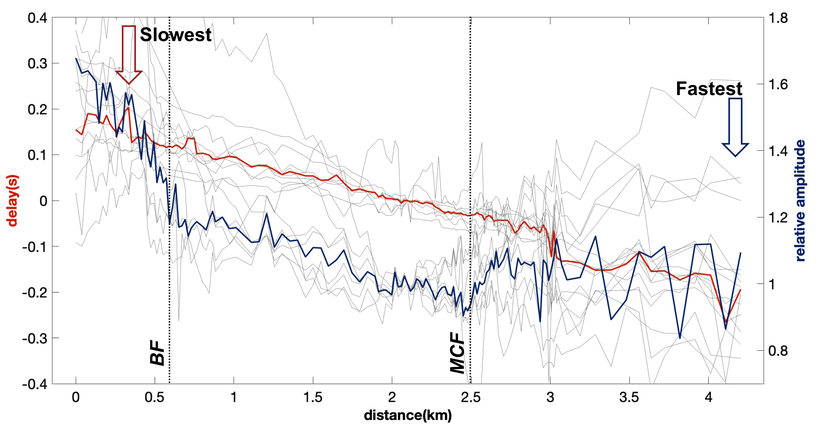

Figure 3: Delay times (after geometry+topography correction) for all regional and teleseismic events (gray lines) using manual P arrival picks (Figure 2), and, the median (dark red line) of all profiles. Maximum amplitudes 1.5 s after P picks for each station (gray lines) and median of all the profile amplitudes (dark blue line).

Local Earthquake Results

The higher frequency energy from local earthquakes near the SSAF allows higher resolution information to be obtained of the internal fault zone in the area.

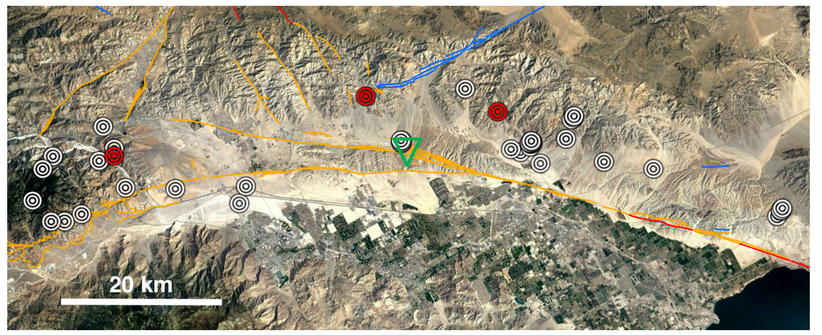

Figure 4: Local SSAF earthquakes from the SCSN catalog analyzed in this study. Waveforms from red circles are shown and analyzed in Figures 5 and 6. Green triangle is the survey site.

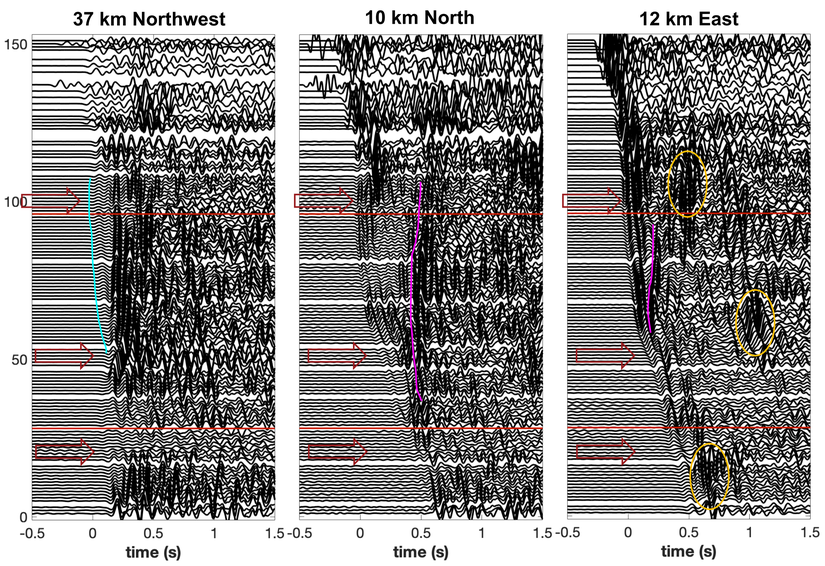

Figure 5: Three example local earthquake P wavefields (15 HZ low-pass filter). In addition to the major structural change around stations 50-60, greater waveforms variability is now also apparent across the BF and MCF (arrows). Potential fault zone head waves (cyan), reflected waves (magenta) and trapped waves (orange) are shown.

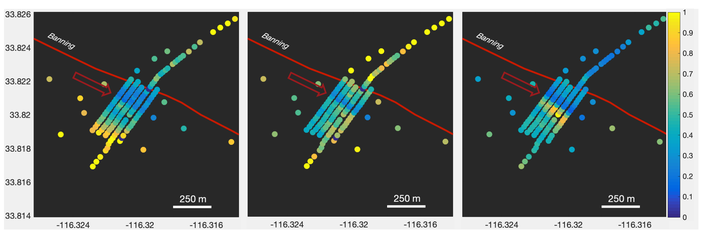

Figure 6: Maximum P amplitude across the BF dense array for the three events in Figure 5.

Summary/Future work

The preliminary results together reveal large-scale structural changes across the MCF, ~200 m SW of the BF and a yet unknown boundary ~400 NE of the BF surface trace (potential damage zone edge), with anomalous amplified ground motion observed around all these boundaries. Future work will include more in-depth analyses of fault zone head, reflected and trapped waves (Figure 5) and the S wavefields from local earthquakes.

Acknowledgements

We would like to thank the IRIS PIC and the University of Utah Seismograph Stations for providing instrumentation for this work and the CNLM Thousand Palms Oasis Preserve and BLM for granting property access. We would also like to acknowledge help during the deployment and retrieval of instrumentation from students, post docs, faculty and staff of various SCEC affiliated institutions, including, USC/SCEC, UCSD/SIO, UU, SDSU, USGS and JPL. We are also very grateful for NSF support.